Persistence of cluster structure in the ground state of ^{11}B

Naoyuki Itagaki,[1] Tomoya Naito,[2,3] and Yuichi Hirata[4]
[1]*Yukawa Institute for Theoretical Physics, Kyoto University, Kitashirakawa Oiwake-Cho, Kyoto 606-8502, Japan*
[2]*Department of Physics, Graduate School of Science, The University of Tokyo, Tokyo 113-0033, Japan*
[3]*RIKEN Nishina Center, Wako 351-0198, Japan*
[4]*Ninomiya, Tsukuba, Ibaraki 305-0051, Japan*

(Received 21 September 2021; accepted 12 January 2022; published 4 February 2022)

Background: The α particles emitted from excited states of ^{12}C could be utilized for cancer treatment and the method is called proton boron capture therapy (PBCT). The α particles are created by a clinical proton beam on the ^{11}B target. The ^{11}B $+p$ threshold corresponds to the excitation energy of 16.0 MeV in ^{12}C, where the excited states decay by emitting α particles.
Purpose: For the nuclear structure side, whether the ground state of ^{11}B contains the seeds of the cluster states is a crucial question. It has been known that one of the noncentral interactions, the spin-orbit interaction, plays a role in nuclear systems of washing out the α clusters; it works as a driving force to stabilize the symmetry of the jj-coupling shell model. It is of special importance to show the persistence of $\alpha + \alpha + t$ cluster configuration in the ground state of ^{11}B.
Methods: In addition to the basis states with cluster configurations, we include their breaking effects by employing the antisymmetrized quasicluster model. The cluster states and shell-model states are treated on the same footing and are coupled.
Results: The inclusion of the breaking effect of $\alpha + \alpha + t$ cluster structure is found to contribute to the lowering of the ground-state energy by about 2 MeV, and cluster structure is slightly broken. The third $3/2^-$ state has been suggested as a cluster state both theoretically and experimentally, and we confirmed the well-developed clustering.
Conclusions: The ground state of ^{11}B can be considered as a seed of the cluster states; it still keeps enough component of $\alpha + \alpha + t$ cluster. Assuming the typical three-α-cluster state of ^{12}C as an equilateral triangular configuration with the relative distances of 3–4 fm, the ground state of ^{11}B is found to have a certain squared overlap with such state when a proton approaches.

DOI: 10.1103/PhysRevC.105.024304

I. INTRODUCTION

In describing the structure of light nuclei, the ^{4}He nucleus is often treated as a subsystem called α cluster due to its large binding energy in the free space. The most famous example of the state comprised of α clusters is the second 0^+ state of ^{12}C called the Hoyle state, which is a three-α state with large relative distances between α clusters [1,2]. The cluster models have been found to be quite effective in describing various properties of such states [3,4].

Cluster states of ^{12}C, which are located higher than the Hoyle state in energy, have recently been considered for cancer treatment. This method is called proton boron capture therapy (PBCT). A clinical proton beam on the ^{11}B target induces excited states of ^{12}C with three-α configurations above the three-α threshold energy, and emitted α particles from these states as they decay are used for destroying cancer cells [5]. For ^{12}C, the ^{11}B $+p$ threshold corresponds to the excitation energy of 16.0 MeV, well above three-α threshold energy of 7.4 MeV, but the neutron threshold (18.7 MeV) is not opened. Therefore, the excited states decay by emitting α particles. The three-α-cluster states of ^{12}C in this energy region have been investigated for decades [6], and the data of p-^{11}B scattering cross section has been accumulated. Recently, the advantage of PBCT was compared with other therapies [7,8]. Also, simulations and experiments have been perform to confirm its reliability and feasibility [9–11].

For the nuclear structure side, it would be still intriguing to investigate whether the $\alpha + \alpha + t$ structure persists in the ground state of ^{11}B. The fact that this method work means that the ground state of ^{11}B contains enough components of the $\alpha + \alpha + t$ cluster configurations, which is the seed of the three-α states of ^{12}C. It has been discussed in ^{11}B that the third $3/2^-$ state is a candidate for the state with a cluster structure [12], but it is considered that in the ground state, the cluster structure is washed out to some extent as in the case of ^{12}C. Indeed, the spin-orbit interaction is known to work as a driving force to break the α clusters [13].

In most of the conventional α-cluster models, the contribution of the noncentral interactions (spin-orbit and tensor interactions) vanishes. If noncentral interaction acts attractively by incorporating shell-model states in the model space,

we must extend the model space and break the cluster structure. As is well known, the spin-orbit interaction is important in the shell model; the observed magic numbers of 28, 50, and 126 correspond to the subclosure configurations of $f_{7/2}$, $g_{9/2}$, and $h_{11/2}$ of the jj-coupling shell model [14].

This spin-orbit contribution is included by extending the cluster model; we have developed the antisymmetrized quasicluster model (AQCM) [15–28]. This method allows us to smoothly transform α-cluster model wave functions to jj-coupling shell-model ones, and we call the clusters that feel the effect of the spin-orbit interaction owing to this model "quasiclusters." We have previously introduced AQCM to ^{12}C and discussed the competition between the cluster states and jj-coupling shell-model state [23]. The consistent description of ^{12}C and ^{16}O, which has been a long-standing problem of microscopic cluster models, has been achieved. Also, not only the competition between the cluster states and the lowest shell-model configuration, the effect of single-particle excitation was further included for the description of the ground state [28].

For ^{11}B, until now, various cluster models [29–32] and antisymmetrized molecular dynamics (AMD) [33,34] have been applied, where the main focus was the clustering in the excited states. In this paper, however, we couple cluster model space and shell-model space and investigate the persistence of the $\alpha+\alpha+t$ cluster configuration in the ground state of ^{11}B. In addition to the basis states with cluster configurations, cluster breaking configurations are prepared with AQCM, where the contribution of the spin-orbit interaction plays an important role. Furthermore, the basis states with the $\alpha+\alpha+3N$ configurations are generated. All of these basis states are superposed based on the framework of the generator coordinate method (GCM), and cluster-shell competition is microscopically investigated. The interactions used are the same as those in our previous analysis on ^{12}C [28]. For the central part, the Tohsaki interaction [35], which has finite range three-body terms, is adopted. There is no free parameter to be adjusted. For the spin-orbit part, we use the spin-orbit term of the G3RS interaction [36], whose strength is set to give a consistent description of ^{12}C and ^{16}O [23].

This paper is organized as follows: The framework is described in Sec. II. The results are shown in Sec. III. The conclusions are presented in Sec. IV.

II. FRAMEWORK

The wave function is fully antisymmetrized, and we superpose three kinds of the basis states: $\alpha+\alpha+t$ basis states (75 bases), AQCM basis states (12 bases), and $\alpha+\alpha+3N$ basis states (48 bases), whose schematic figure is shown in Fig. 1. All these states are superposed based on the GCM after the angular-momentum projection and amplitude for each basis state is determined by diagonalizing the norm and Hamiltonian matrices.

A. Single-particle wave function

In our framework, each single particle is described by a Gaussian form as in many other cluster models, including the Brink model [37],

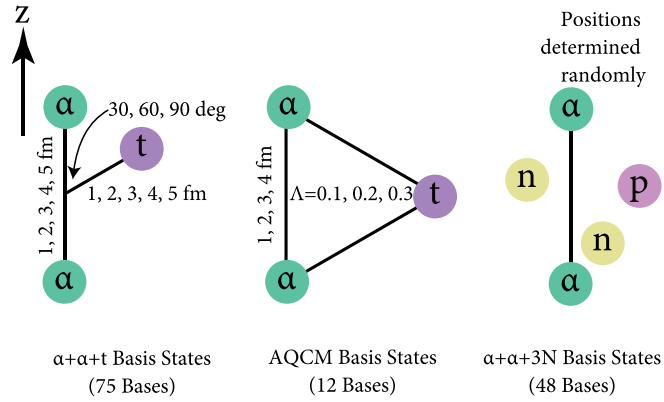

FIG. 1. Schematic figure of basis sets used in this work. See the text for more detail.

$$\phi^{\tau,\sigma}(\boldsymbol{r}) = \left(\frac{2\nu}{\pi}\right)^{\frac{3}{4}} \exp[-\nu(\boldsymbol{r}-\boldsymbol{\zeta})^2]\chi^{\tau,\sigma}, \tag{1}$$

where the Gaussian center parameter $\boldsymbol{\zeta}$ is related to the expectation value of the position of the nucleon, and $\chi^{\tau,\sigma}$ is the spin-isospin part of the wave function. For the size parameter ν, here we use $\nu = 0.23$ fm^{-2}, which gives the optimal 0^+ energy of ^{12}C within a single AQCM basis state. The Slater determinant is constructed from these single-particle wave functions by antisymmetrizing them.

B. Basis states of $\alpha+\alpha+t$ cluster configurations

When four single-particle wave functions with different spin and isospin share a common $\boldsymbol{\zeta}$ value, an α cluster is formed. Similarly, when two neutrons with opposite spin orientations and a proton share the same $\boldsymbol{\zeta}$, a triton cluster is formed. We prepare 75 basis states with different $\alpha+\alpha+t$ configurations. The distance between two α clusters is changed from 1 fm to 5 fm in the step of 1 fm. The triton is set at the places with the distance of 1–5 fm from the center of two α clusters, which is changed in the step of 1 fm, and the axis measured from the α-α axis is set to 30°, 60°, and 90°. In all these states, the $\boldsymbol{\zeta}$ values in Eq. (1) are real numbers.

C. Basis states of antisymmetrized quasicluster model

This cluster wave function is transformed into jj-coupling shell model based on the AQCM, by which the contribution of the spin-orbit interaction due to the breaking of α clusters is included. Here the $\boldsymbol{\zeta}$ values in Eq. (1) are changed to complex numbers. When the original value of the Gaussian center parameter $\boldsymbol{\zeta}$ is $\boldsymbol{R}$, which is real and related to the spatial position of this nucleon, it is transformed by adding the imaginary part as

$$\boldsymbol{\zeta} = \boldsymbol{R} + i\Lambda \boldsymbol{e}^{\text{spin}} \times \boldsymbol{R}, \tag{2}$$

where $\boldsymbol{e}^{\text{spin}}$ is a unit vector for the intrinsic-spin orientation of this nucleon. The control parameter Λ is associated with the breaking of the cluster, and two nucleons with opposite spin orientation have $\boldsymbol{\zeta}$ values that are complex conjugates of each

other. This situation corresponds to the time-reversal motion of two nucleons. After this transformation, the α clusters are called quasiclusters.

In our previous analysis on ^{12}C, we have prepared three quasiclusters with an equilateral triangular shape. We introduced two parameters, R representing the α-α distances and Λ for the breaking of the α clusters. The subclosure configuration of $(s_{1/2})^2\,(p_{3/2})^4$ of the jj-coupling shell model can be obtained at the limit of $R \to 0$ and $\Lambda = 1$.

For ^{11}B, we remove one spin-down proton from a quasicluster. The R and Λ values are taken as $R = 1, 2, 3, 4$ fm and $\Lambda = 0.1, 0.2, 0.3$ ($\Lambda = 0$ states are not necessary because they have large overlaps with the $\alpha + \alpha + t$ basis states).

It has been discussed that the cluster model space covers the model space of the shell model, if the wave function is antisymmetrized and we take the small-distance limit between clusters. This statement is correct when the term of the "shell model" is used in the sense of the three-dimensional harmonic-oscillator. The cluster-model wave function becomes the three-dimensional harmonic-oscillator one at the limit of the small relative distances. However, the three-dimensional harmonic-oscillator wave function (corresponding to $\Lambda = 0$ in AQCM) is quite different from the jj-coupling shell-model one (corresponding to $\Lambda = 1$ in AQCM), as we can easily assess using our AQCM. Figure 2(a) shows the squared overlap between the three-dimensional harmonic oscillator wave function (cluster model with small distances) and AQCM one as functions of the Λ value. The dotted line is for ^{12}C with equilateral triangular configuration and very small distances between three quasiclusters. The vertical axis shows the squared overlap between $\Lambda = 0$ and finite-Λ states. The angular momentum and parity are projected to 0^+. The dotted line rapidly drops and the state with $\Lambda = 0$ (identical to the three-dimensional harmonic-oscillator state) has very small squared overlap with the subclosure configuration of the jj-coupling shell model $[(s_{1/2})^4\,(p_{3/2})^8]$ of about 5 % at $\Lambda = 1$. The solid line is for the $3/2^-$ of ^{11}B. Since one proton is missing compared with ^{12}C, the squared overlap between the three-dimensional harmonic-oscillator and jj-coupling shell model increases, but the value is still quite small (slightly above 10 %).

Next, the squared overlaps between a typical three-α-cluster state and AQCM basis states are shown in Fig. 2(b). Here, the typical three-α-cluster state means an equilateral triangular configuration with the α-α distance (R) of 4 fm. The solid and dotted lines are for the squared overlap with this typical cluster state and the AQCM basis states with $R = 2$ fm and $R = 3$ fm as functions of Λ, respectively. In our previous work, we have discussed that $R = 2.0$ fm and $\Lambda = 0.2$ is the optimal AQCM basis state, which is found have the squared overlap of 10 % with the typical cluster state.

D. Basis states of $\alpha + \alpha + 3N$

To describe the single-particle nature of three nucleons outside two α clusters, we prepare $\alpha + \alpha + 3N$ basis states, where α-α distance is determined using the random number (between 0–5 fm with equal probability) and positions of three nucleons (a spin-up proton and two neutrons with opposite spin directions) are also determined randomly. We generate 48 basis states and include them in the diagonalization process of the norm and Hamiltonian matrices.

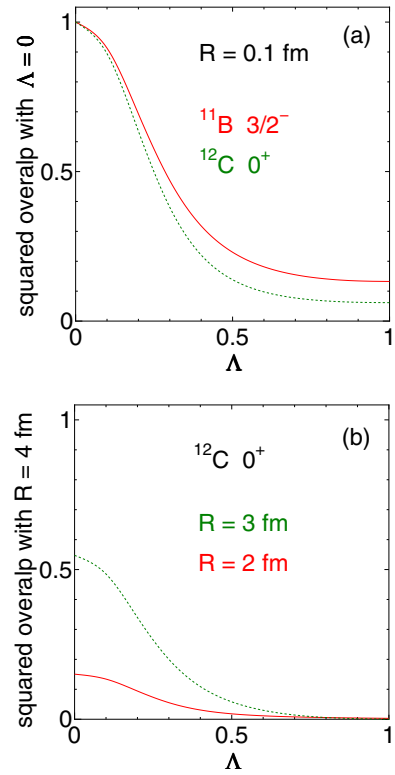

FIG. 2. (a) Squared overlap between the three-dimensional harmonic oscillator (shell-model) wave function and AQCM one as functions of the Λ value. The dotted line is for the 0^+ state of ^{12}C between equilateral triangular configuration and very small distances between three quasiclusters and finite-Λ states. The solid line is for the $3/2^-$ of ^{11}B. (b) Squared overlaps between a typical three-α-cluster state ($R = 4$ fm) and AQCM basis states. The solid and dotted lines are for the squared overlap with this typical cluster state and the AQCM basis stats with $R = 2$ fm and $R = 3$ fm as functions of Λ, respectively.

E. J^π projection and generator coordinate method

As we have mentioned before, totally we generate 135 intrinsic states. The basis states from 1 to 75 are $\alpha + \alpha + t$ states with various configurations, those from 76 to 87 are AQCM basis states with $R = 1, 2, 3, 4$ fm and $\Lambda = 0.1, 0.2, 0.3$, and those from 88 to 135 are $\alpha + \alpha + 3N$ configurations with the α-α distance of 0–5 fm. These 135 basis states are numerically projected to eigenstates of angular momentum and parity. After the angular-momentum projection, different K number states are generated from the same intrinsic basis state. Here, the z direction of the intrinsic frame is parallel to the axis of two α (quasi) clusters. These different K states are treated independently when we determine the coefficients for the linear combination of the basis states based on GCM. Therefore, after the angular-momentum projection, the number of the basis states increases to 540, the basis states of 1–135, 136–270, 271–405, and 406–540 are $K = 1/2$, $K = 3/2$, $K = -1/2$, and $K = -3/2$, respectively.

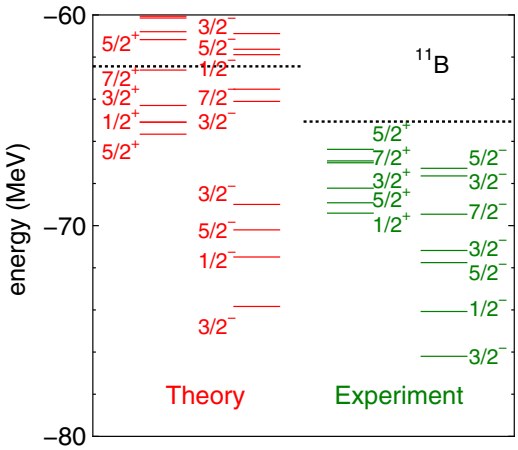

FIG. 3. Energy levels of ^{11}B. The 135 basis states are projected to the eigenstates of angular momentum and parity, and basis states with $K = 1/2, 3/2, -1/2$, and $-3/2$ are independently treated when diagonalizing the norm and Hamiltonian matrices based on GCM. Dotted lines are threshold energies of $\alpha + \alpha + t$.

F. Hamiltonian

The Hamiltonian consists of the kinetic-energy and potential-energy terms. For the potential part, the interaction consists of the central, spin-orbit, and Coulomb terms. The interactions are the same as those in our previous analysis on ^{12}C [28]. For the central part, the Tohsaki interaction [35] is adopted. This interaction has finite-range three-body terms in addition to two-body terms, which is designed to reproduce both saturation properties and scattering phase shifts of two α clusters. For the spin-orbit part, there is no free parameter left for each nucleus for this interaction. For the spin-orbit part, we use the spin-orbit term of the G3RS interaction [36], which is a realistic interaction originally developed to reproduce the nucleon-nucleon scattering phase shifts. The strength of the spin-orbit interactions is set to $V^1_{ls} = V^2_{ls} = 1800$ MeV, which allows consistent description of ^{12}C and ^{16}O [23].

III. RESULTS

A. Energy levels of ^{11}B

We project 135 basis states to the eigenstates of angular momentum and parity, and basis states with $K = 1/2$, $3/2$, $-1/2$, and $-3/2$ are independently treated. Thus, based on the GCM, we diagonalize the norm and Hamiltonian matrices with the dimension of 540. The obtained energy levels of ^{11}B are listed in Fig. 3, where dotted lines are the threshold energies of $\alpha + \alpha + t$. The ground $3/2^-$ state is obtained at -73.84 MeV, compared with the experimental value of -76.20 MeV. Although we have no adjustable parameter for the central interaction and the spin-orbit strength is determined in our previous work for ^{12}C, the absolute value of the calculated ^{11}B energy is quite reasonable.

The theoretical binding energy underestimates the experimental one by 2.4 MeV, but the agreement between theoretical and experimental binding energies becomes even better if we measure them from the $\alpha + \alpha + t$ threshold.

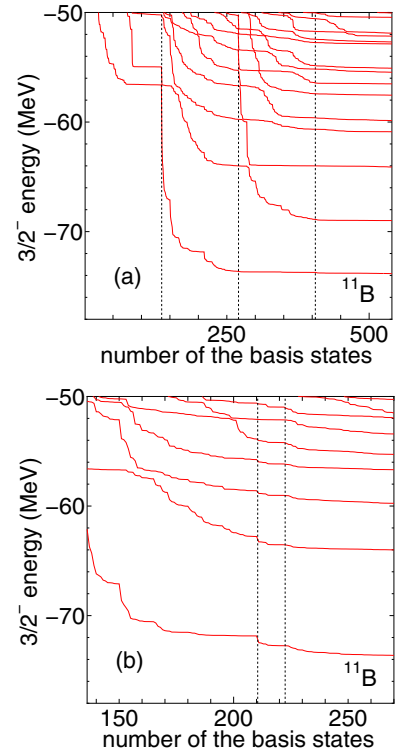

FIG. 4. Energy convergence of $3/2^-$ states of ^{11}B. The horizontal axis shows the number of the basis states. (a) 135 basis states are projected to $K = 1/2$ (1–135 on the horizontal axis), $K = 3/2$ (136–270), $K = -1/2$ (271–405), and $K = -3/2$ (406–540). (b) Excerpt of the $K = 3/2$ part.

This is because the underestimation can be absorbed in the internal energies of the clusters; the theoretical value of α (triton) energy is -27.31 MeV (-7.82 MeV), compared with the experimental value of -28.29 MeV (-8.48 MeV). The ground-state energy of ^{11}B is -11.40 MeV from the $\alpha + \alpha + t$ threshold compared with the experimental value of -11.20 MeV.

B. Energy convergence of the $3/2^-$ states

The energy convergence of the $3/2^-$ states of ^{11}B is shown in Fig. 4(a). The horizontal axis shows the number of the basis states superposed in the GCM calculation. As mentioned before, we generated 135 basis states, which are projected to the J^π eigenstates with $K = 1/2, 3/2, -1/2$, and $-3/2$, and thus we diagonalize the norm and Hamiltonian with the dimension of $135 \times 4 = 540$. From this figure, the first and third $3/2^-$ states are found to have predominantly the $K = 3/2$ component, whereas the second $3/2^-$ state has mainly the $K = -1/2$ component. Figure 4(b) is the excerpt of the $K = 3/2$ part. Here the first 75 basis states (136–210 on the horizontal axis) are basis states with the $\alpha + \alpha + t$ cluster configurations, the next 12 basis states (211–222) are AQCM, and the last 48 basis states (223–270) are $\alpha + \alpha + 3N$ configurations.

From these figures, we can confirm that the inclusion of the breaking effect of $\alpha + \alpha + t$ cluster structure contributes to the lowering of the ground-state energy by about 2 MeV

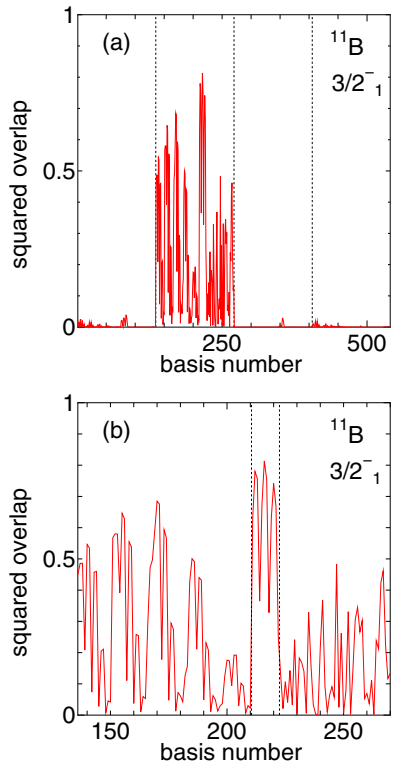

FIG. 5. Squared overlap between the ground $3/2^-$ state and each basis state. (a) Basis states with $K = 1/2$ (1–135 on the horizontal axis), $K = 3/2$ (136–270), $K = -1/2$ (271–405), and $K = -3/2$ (406–540). (b) Excerpt of the $K = 3/2$ part.

[for instance, we can compare the energies at 210 and 270 on the horizontal axis of Fig. 4(b)]. The decrease of the energy when cluster breaking is incorporated is about half compared with ^{12}C, where the spin-orbit effect decreases the ground-state energy by several MeV (the same interaction is applied to ^{12}C in Ref. [23]). This is because the spin-orbit interaction acts for a proton in the triton cluster already within the $\alpha + \alpha + t$ model space; the antisymmetrization effect excites the triton cluster with the $(0s)^3$ configuration to the p shell and the angular-momentum projection allows the change of this proton wave function to $p_{3/2}$. Anyhow, two α clusters and a dineutron cluster in the triton cluster are free from the spin-orbit interaction, and breaking these clusters based on the AQCM has a certain effect of decreasing the ground state by about 2 MeV.

C. Squared overlap with each basis state

Figure 5(a) shows the squared overlap between the ground $3/2^-$ state and each basis state. Here, basis states with $K = 1/2$ correspond to 1–135 on the horizontal axis, and $K = 3/2$, $K = -1/2$, and $K = -3/2$ correspond to 136–270, 271–405, and 406–540 on the horizontal axis. As expected, the contribution of $K = 3/2$ is dominant in the ground state.

Figure 5(b) is the excerpt of the $K = 3/2$ part. As in the previous figure, the first 75 basis states (136–210 on the horizontal axis) are basis states with the $\alpha + \alpha + t$ cluster configurations, the next 12 basis states (211–222) are AQCM, and the last 48 basis states (223–270) are $\alpha + \alpha + 3N$ configurations. For the $\alpha + \alpha + t$ cluster configurations basis states (136–210), we see five peak structures, and the basis states are classified into five groups with the interval of 15 basis states (136–150, 151–165, 166–180, 181–195, and 196–210). These five groups correspond to the basis states with the α-α distances of 1, 2, 3, 4, and 5 fm, and as we can see, α-α distance of 3 fm contributes the most importantly (166–180). These 15 basis states are further classified into five groups with the interval of three (166–168, 169–171, 172–174, 175–177, and 178–180) corresponding to the position of the triton at 1, 2, 3, 4, and 5 fm from the center of α-α. The largest squared overlap of 0.68 within the $\alpha + \alpha + t$ cluster configurations is given for the basis state 170 on the horizontal axis, which corresponds to the α-α distance is 3 fm, and the triton is located at 2 fm from the center of α-α with the angle of 30°. We tried the case with much smaller steps for the mesh points of GCM and found the optimal $\alpha + \alpha + t$ basis state, but the obtained squared overlap with the optimal $\alpha + \alpha + t$ basis state and the final solution does not change. Therefore, the ground state is found to have the $\alpha + \alpha + t$ component of about 70 %.

Furthermore, we can get insight about the overlap with the higher excited cluster states of ^{12}C when a proton is added, which is important medically, as explained in the introduction. Such cluster states can be characterized as a state with the three-α clusters with the relative distances of ≈4 fm, since the α-α system has the minimum energy with such relative distance in the free space. In our calculation, the basis states 181–195 correspond to the α-α distance of 4 fm, and in the basis states 190–192, the last α cluster is placed at 4 fm from the center of two α clusters. We can confirm that the ground state has the squared overlap of about 50 % with those basis states, proving it contains enough amount of seeds for the Hoyle state of ^{12}C.

However, the figures show that the AQCM basis states (211–222) describe the ground state better than the $\alpha + \alpha + t$ cluster configuration and they are more important. These AQCM basis states are classified into three groups with the interval of four, and basis states 211–214 are for $\Lambda = 0.1$ (215–218 are for $\Lambda = 0.2$ and 219–222 are for $\Lambda = 0.3$). The largest squared overlap of 0.81 is given for the basis state 216 on the horizontal line corresponding to the basis states with $\Lambda = 0.2$ and $R = 2$ fm, where R represents the distances between quasiclusters with equilateral triangular shape. The AQCM basis states with finite-Λ values have larger squared overlaps than the $\alpha + \alpha + t$ cluster configurations, and this means that the breaking of clusters due to the spin-orbit contribution is important. In our previous work on ^{12}C with the same interaction, similarly, $\Lambda = 0.2$ was found to give the optimal energy, where the α-α distance was reduced to 2 fm owing to the strong attraction of three quasiclusters.

Figure 6(a) shows the squared overlap between the second $3/2^-$ state and each basis state. The orders of the basis states are the same as in the previous figures, and it is obvious that $K = -1/2$ is important for this state. In our basis states, the spin direction of a valence proton is set to spin up, and thus $K = -1/2$ means that the orbital angular momentum of the proton and its spin are antiparallel, for which the spin-orbit in-

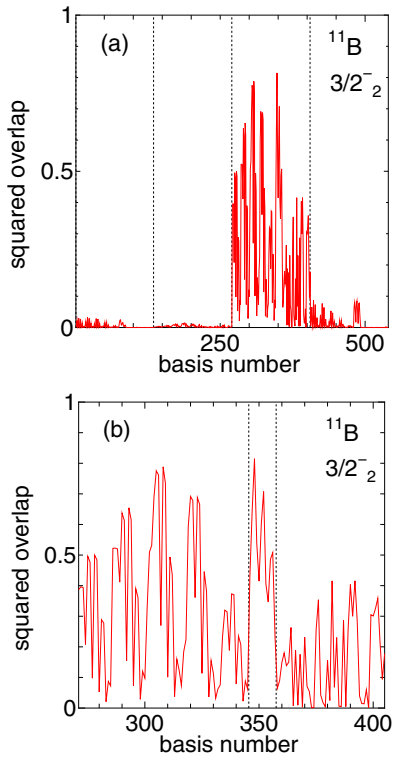

FIG. 6. Squared overlap between the second $3/2^-$ state and each basis state. (a) Basis states with $K = 1/2$ (1–135 on the horizontal axis), $K = 3/2$ (136–270), $K = -1/2$ (271–405), and $K = -3/2$ (406–540). (b) excerpt of the $K = -1/2$ part.

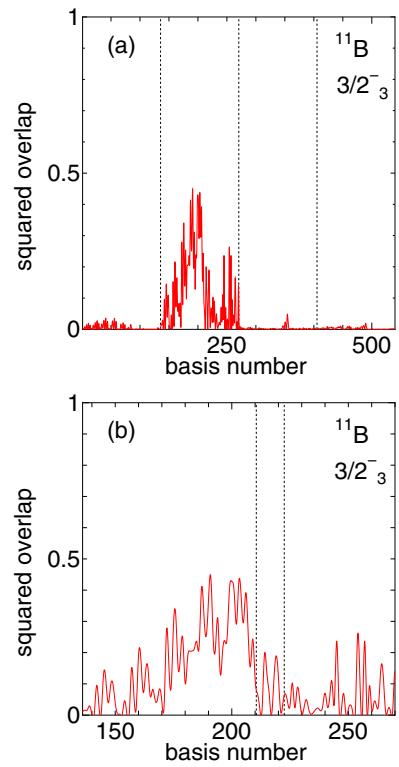

FIG. 7. Squared overlap between the third $3/2^-$ state and each basis state. (a) Basis states with $K = 1/2$ (1–135 on the horizontal axis), $K = 3/2$ (136–270), $K = -1/2$ (271–405), and $K = -3/2$ (406–540). (b) Excerpt of the $K = 3/2$ part.

teraction acts repulsively. Figure 6(b) is the excerpt of the $K = -1/2$ part. The squared overlaps with the $\alpha + \alpha + t$ cluster states (271–345 on the horizontal axis) increase compared with the previous cases of the ground state, and, again, the α-α distance of 3 fm is found to be most important among them. However, the squared overlaps with the AQCM basis states (346–357 on the horizontal axis) have even larger overlaps. Contrary to the ground-state case, the basis state with $\Lambda = 0.1$ has the largest squared overlap.

Figure 7(a) shows the squared overlap between the third $3/2^-$ state, which has been suggested as a candidate for the cluster state both theoretically and experimentally, and each basis state. Here, we find that the contribution of $K = 3/2$ is dominant, and Fig. 7(b) is the excerpt of the $K = 3/2$ part. The squared overlaps with the $\alpha + \alpha + t$ cluster states (136–210 on the horizontal axis) are much larger than those of the AQCM basis states (211–222). We can confirm that the breaking effect of clusters is small and this state is really a cluster state, as expected. The α-α distance of 4 fm is found to have the largest overlap, which can be considered as well-developed clustering.

Summarizing, one can find that $K = 3/2$ contributes dominantly to the ground $3/2^-$, where AQCM states dominates the most, especially with $\Lambda = 0.2$, while the $\alpha + \alpha + t$ cluster states, especially with α-α distance 3 fm, contributes largely as well; $K = -1/2$ contributes dominantly to the second $3/2^-$, where AQCM states dominates the most, especially with $\Lambda = 0.1$, while the $\alpha + \alpha + t$ cluster states, especially with α-α distance 3 fm, contributes largely as well; $K = 3/2$ contributes dominantly to the third $3/2^-$, where the $\alpha + \alpha + t$ cluster states, especially with α-α distance 4 fm, dominates.

D. Matter root-mean-square radii

The matter root-mean-square (rms) radii of the $3/2^-$ and $1/2^+$ states obtained with the present calculation are shown in the column "Present" in Table I together with AMD [12], the orthogonal condition model (OCM) [31], the Brink model GCM (B-GCM) [32], and experiment (Expt.). For the $3/2^-$ states, there is no large difference and our results are consistent with other previous works. Anyway, the third $3/2^-$ state has a large radius. For the $1/2^+$ states, our results are

TABLE I. Matter root-mean-square (rms) radii of the $3/2^-$ and $1/2^+$ states obtained with the present calculation (Present) together with AMD [12], OCM [31], Brink model GCM (B-GCM) [32], and experiment (Expt.). All units are fm.

State	Present	AMD	OCM	B-GCM	Expt.
$3/2^-_1$	2.37	2.29	2.22	2.38	2.09 ± 0.12
$3/2^-_2$	2.57	2.46	2.23	2.64	
$3/2^-_3$	2.70	2.65	3.00	2.99	
$1/2^+_1$	2.91		2.82	2.91	
$1/2^+_2$	2.88		5.93	2.88	

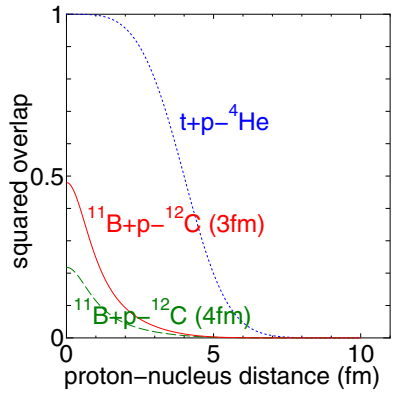

FIG. 8. Squared overlap between proton-^{11}B and three-α-cluster states of ^{12}C as a distance between them. The solid and dashed lines are for the three-α-cluster states with the relative α-α distances of 3 fm and 4 fm, respectively, where the angular momentum is projected to 2^+. The dotted line is for the one between proton-triton and ^{4}He (angular momentum is 0^+).

consistent with the B-GCM results. The OCM gives very large radius for $1/2^+_2$, and we need larger model space for the purpose of checking this result.

E. Squared overlap between $p + {}^{11}$B and ^{12}C

We have shown how the components of the $\alpha + \alpha + t$ configurations are mixed in the ground state of ^{11}B. Here, finally, we discuss the squared overlap with the three-α-cluster configuration of ^{12}C when a proton approaches ^{11}B. We start with the case of single-α formation. The dotted line in Fig. 8 shows the squared overlap between an α particle and $t + p$ as a function of the distance between the triton cluster and the proton. The total angular momentum is projected to 0^+. Here the spin orientations of the proton and the one in the triton cluster are assumed to be antiparallel. The squared overlap becomes zero when they are parallel. Therefore, we need an additional factor of $1/2$, which is not considered in Fig. 8, in the real situation of the proton scattering, where spin orientations are not fixed. The squared overlap between α and $t + p$ is unity at zero-distance and gradually drops as the distance increases.

Next, the dashed line shows the squared overlap between $p + {}^{11}$B and three-α-cluster states of ^{12}C as a function of the distance between the proton and ^{11}B. In the real situation of the proton scattering, various three-α-cluster states of ^{12}C are created when the proton meets ^{11}B, and in this calculation, such three-α-cluster states are represented by a single configuration of an equilateral triangular shape with the relative α-α distance of 4 fm (optimal α-α distance of ^{8}Be in the free space). The target nucleus, ^{11}B, is represented by the most important basis state in the previous section; AQCM basis state with $R = 3$ fm and $\Lambda = 0.2$. To compare with the real situation of the proton scattering, the target nucleus of ^{11}B should be angular-momentum projected to $3/2^-$ and the relative angular momentum between p and ^{11}B must also be treated as a good quantum number. However, here these are approximated as the total angular-momentum projection, and the proton is assumed to approach from the perpendicular direction to the three quasiclusters. The threshold energy of $^{11}\mathrm{B} + p$ corresponds to $E_x = 15.956\,68$ MeV in ^{12}C, and the resonances slightly above this energy are clinically important sources of the α-cluster emission. According to the database at National Nuclear Data Center, the 2^+ resonance state of ^{12}C at $E_x = 16.106\,08$ MeV α decays with the branching ratio of 100 %. Therefore, here we project the angular momentum to 2^+, and in this case, the relative wave function between the proton and ^{11}B dominantly has the p-wave component. Again the spin orientations of the incident proton and that in the target nucleus are assumed to be antiparallel, and thus we need an additional factor of $1/2$, which is not considered in Fig. 8, to compare with the real situation. We can see the squared overlap of 10%–20 % at small distances. The value is not very large, but the proton scattering on ^{11}B is considered to have a sizable branching ratio for creating the three-α-cluster states. However, it is not necessary to restrict the α-α distance for the typical cluster state to 4 fm. When we change the α-α distances of ^{12}C to 3 fm as the example of typical cluster state, which is the optimal distance within the three-α-cluster model, the squared overlap is almost doubled (solid line).

IV. CONCLUSIONS

Proton boron capture therapy (PBCT) is a promising technique for cancer treatment. By injecting a clinical proton beam to ^{11}B in human body, highly excited states of ^{12}C are created, and the emitted α particles are expected to destroy cancer cells. In ^{12}C, the $^{11}\mathrm{B} + p$ threshold corresponds to the excitation energy of 16.0 MeV, which is below the neutron threshold but above the three-α threshold, and thus three-α emission is the only possible decay mode except for proton emission. There exist some states in this energy region whose main decay modes are α emission.

From the nuclear structure point of view, it is quite intriguing to investigate whether the $\alpha + \alpha + t$ structure persists in the ground state of ^{11}B as a seed of three α particles. This is because the cluster structure would be washed out to some extent as in the case of ^{12}C; the spin-orbit interaction is known to work as a driving force to break the α clusters and strengthen the symmetry of jj-coupling shell model.

We have discussed the persistence of $\alpha + \alpha + t$ cluster configuration in the ground state of ^{11}B. Although this effect is not investigated within the traditional α-cluster models, the antisymmetrized quasicluster model (AQCM) allows us to transform cluster model wave functions to jj-coupling shell-model wave functions, by which the contribution of the spin-orbit interaction can be included. All of these basis states are superposed based on the framework of the generator coordinate method (GCM), and cluster-shell competition is microscopically investigated.

It is confirmed that the inclusion of the breaking effect of $\alpha + \alpha + t$ cluster structure contributes to the lowering of the ground-state energy by about 2 MeV. The decrease of the energy when cluster breaking is incorporated is about half compared with ^{12}C, where the spin-orbit effect decreases the ground-state energy by several MeV, and this is be-

cause the spin-orbit interaction acts for a proton in the triton cluster already within the $\alpha + \alpha + t$ model space; the antisymmetrization effect on the triton cluster to the p shell and the angular-momentum projection allows the change of this proton wave function to $p_{3/2}$. Anyway, two α clusters and a dineutron cluster in the triton cluster are free from the spin-orbit interaction, and breaking these clusters based on AQCM has a certain effect. Nevertheless, the ground state has the $\alpha + \alpha + t$ component of about 70 %. Furthermore, we can get insight that ^{11}B contains the seeds of the Hoyle state of ^{12}C when a proton is added. The three-α-cluster state in highly excited states can be characterized as a state with the three-α clusters with the relative distances of $\approx$4 fm (optimal α-α distance of ^{8}Be in the free space). We can confirm that the ground state of ^{11}B has a certain squared overlap (10%–20 %) with the state having the α-α distance of 4 fm when a proton approaches. When we change the α-α distances of ^{12}C to 3 fm as the example of typical cluster state, the squared overlap is almost doubled.

The third $3/2^-$ state has been suggested as a cluster state both theoretically and experimentally. The squared overlaps with the $\alpha + \alpha + t$ cluster states are much larger than the AQCM basis states. The α-α distance of 4 fm is found to have the largest overlap, which can be considered as well-developed clustering.

ACKNOWLEDGMENTS

This work was supported by JSPS KAKENHI Grant No. 19J20543. The numerical calculations have been performed using the computer facility of the Yukawa Institute for Theoretical Physics, Kyoto University (Yukawa-21).

[1] F. Hoyle, On nuclear reactions occurring in very hot stars. I. The synthesis of elements from carbon to nickel, Astrophys. J., Suppl. Ser. **1**, 121 (1955).
[2] M. Freer and H. O. U. Fynbo, The Hoyle state in ^{12}C, Prog. Part. Nucl. Phys. **78**, 1 (2014).
[3] Y. Fujiwara, H. Horiuchi, K. Ikeda, M. Kamimura, K. Katō, Y. Suzuki, and E. Uegaki, Chapter II. Comprehensive study of alpha-nuclei, Prog. Theor. Phys. Suppl. **68**, 29 (1980).
[4] A. Tohsaki, H. Horiuchi, P. Schuck, and G. Röpke, Alpha Cluster Condensation in ^{12}C and ^{16}O, Phys. Rev. Lett. **87**, 192501 (2001).
[5] G. A. P. Cirrone, L. Manti, D. Margarone *et al.*, First experimental proof of proton boron capture therapy (PBCT) to enhance protontherapy effectiveness., Sci. Rep. **8**, 1141 (2018).
[6] S. Stave III, M. W. Ahmed, R. H. France, S. S. Henshaw, B. Müller, B. A. Perdue, R. M. Prior, M. C. Spraker, and H. R. Weller, Understanding the ^{11}B$(p, \alpha)\alpha\alpha$ reaction at the 0.675 MeV resonance, Phys. Lett. B **696**, 26 (2011).
[7] Z. Ahmadi Ganjeh and M. Eslami-Kalantari, Investigation of proton–boron capture therapy vs. proton therapy, Nucl. Instrum. Methods Phys. Res., Sect. A **977**, 164340 (2020).
[8] N. Khaledi, X. Wang, R. B. Hosseinabadi, and F. Samiei, Is the proton–boron fusion therapy effective?, J. Radiother. Pract. **20**, 153 (2021).
[9] H. J. Meyer, U. Titt, and R. Mohan, Technical note: Monte Carlo study of the mechanism of proton–boron fusion therapy, Med. Phys. **49**, 579 (2022).
[10] M.-S. Kim, M. Wai-Ming Law, S.-K. Djeng, H.-B. Shin, M.-G. Choi, Y.-J. Kim, B.-Y. Choe, T. S. Suh, and D.-K. Yoon, Synergy effect of alpha particles by using natural boron in proton therapy: Computational verification, AIP Adv. **9**, 115017 (2019).
[11] F. A. Geser and M. Valente, Analytical approach to the reaction cross section of the fusion of protons with boron isotopes aimed at cancer therapy, Appl. Radiat. Isot. **151**, 96 (2019).
[12] T. Kawabata, H. Akimune, H. Fujita, Y. Fujita, M. Fujiwara, K. Hara, K. Hatanaka, M. Itoh, Y. Kanada-En'yo, S. Kishi, K. Nakanishi, H. Sakaguchi, Y. Shimbara, A. Tamii, S. Terashima, M. Uchida, T. Wakasa, Y. Yasuda, H. Yoshida, and M. Yosoi, $2\alpha + t$ cluster structure in ^{11}B, Phys. Lett. B **646**, 6 (2007).
[13] N. Itagaki, S. Aoyama, S. Okabe, and K. Ikeda, Cluster-shell competition in light nuclei, Phys. Rev. C **70**, 054307 (2004).
[14] M. G. Mayer and H. G. Jensen, *Elementary Theory of Nuclear Shell Structure* (John Wiley, Sons, New York, Chapman Hall, London, 1955).
[15] N. Itagaki, H. Masui, M. Ito, and S. Aoyama, Simplified modeling of cluster-shell competition, Phys. Rev. C **71**, 064307 (2005).
[16] H. Masui and N. Itagaki, Simplified modeling of cluster-shell competition in carbon isotopes, Phys. Rev. C **75**, 054309 (2007).
[17] T. Yoshida, N. Itagaki, and T. Otsuka, Appearance of cluster states in ^{13}C, Phys. Rev. C **79**, 034308 (2009).
[18] N. Itagaki, J. Cseh, and M. Płoszajczak, Simplified modeling of cluster-shell competition in ^{20}Ne and ^{24}Mg, Phys. Rev. C **83**, 014302 (2011).
[19] T. Suhara, N. Itagaki, J. Cseh, and M. Płoszajczak, Novel and simple description for a smooth transition from α-cluster wave functions to jj-coupling shell model wave functions, Phys. Rev. C **87**, 054334 (2013).
[20] N. Itagaki, H. Matsuno, and T. Suhara, General transformation of α cluster model wave function to jj-coupling shell model in various $4N$ nuclei, Prog. Theor. Exp. Phys. **2016**, 093D01 (2016).
[21] H. Matsuno, N. Itagaki, T. Ichikawa, Y. Yoshida, and Y. Kanada-En'yo, Effect of ^{12}C $+\alpha$ clustering on the $E0$ transition in ^{16}O, Prog. Theor. Exp. Phys. **2017**, 063D01 (2017).
[22] H. Matsuno and N. Itagaki, Effects of cluster-shell competition and BCS-like pairing in ^{12}C, Prog. Theor. Exp. Phys. **2017**, 123D05 (2017).
[23] N. Itagaki, Consistent description of ^{12}C and ^{16}O using a finite-range three-body interaction, Phys. Rev. C **94**, 064324 (2016).
[24] N. Itagaki and A. Tohsaki, Nontrivial origin for the large nuclear radii of dripline oxygen isotopes, Phys. Rev. C **97**, 014307 (2018).
[25] N. Itagaki, H. Matsuno, and A. Tohsaki, Explicit inclusion of the spin-orbit contribution in the Tohsaki-Horiuchi-Schuck-Röpke wave function, Phys. Rev. C **98**, 044306 (2018).
[26] N. Itagaki, A. V. Afanasjev, and D. Ray, Possibility of ^{14}C cluster as a building block of medium-mass nuclei, Phys. Rev. C **101**, 034304 (2020).

[27] N. Itagaki, T. Fukui, J. Tanaka, and Y. Kikuchi, ^{8}He and ^{9}Li cluster structures in light nuclei, Phys. Rev. C **102**, 024332 (2020).

[28] N. Itagaki and T. Naito, Consistent description for cluster dynamics and single-particle correlation, Phys. Rev. C **103**, 044303 (2021).

[29] H. Nishioka, S. Saito, and M. Yasuno, Structure study of $2\alpha + t$ system by the orthogonality condition model, Prog. Theor. Phys. **62**, 424 (1979).

[30] P. Descouvemont, The ^{7}Be$(\alpha,\gamma)^{11}$C and ^{7}Li$(\alpha,\gamma)^{11}$B reactions in a microscopic three-cluster model, Nucl. Phys. A **584**, 532 (1995).

[31] T. Yamada and Y. Funaki, $\alpha + \alpha + t$ cluster structures and ^{12}C(0_2^+)-analog states in ^{11}B, Phys. Rev. C **82**, 064315 (2010).

[32] B. Zhou and M. Kimura, $2\alpha + t$ cluster structure in ^{11}B, Phys. Rev. C **98**, 054323 (2018).

[33] Y. Kanada-En'yo, Negative parity states of ^{11}B and ^{11}C and the similarity with ^{12}C, Phys. Rev. C **75**, 024302 (2007).

[34] T. Suhara and Y. Kanada-En'yo, Cluster structures in ^{11}B, Phys. Rev. C **85**, 054320 (2012).

[35] A. Tohsaki, New effective internucleon forces in microscopic α-cluster model, Phys. Rev. C **49**, 1814 (1994).

[36] R. Tamagaki, Potential models of nuclear forces at small distances, Prog. Theor. Phys. **39**, 91 (1968).

[37] D. M. Brink, in *Proceedings of the International School of Physics "Enrico Fermi", Course 36* (Academic Press, New York, London, 1966), p. 247.